

## ARTICLES

**Theory of the Seebeck coefficient in  $\text{LaCrO}_3$  and related perovskite systems**

D. B. Marsh and P. E. Parris

*Department of Physics and the Electronic Materials Institute, University of Missouri–Rolla, Rolla, Missouri 65409*

(Received 14 March 1996; revised manuscript received 6 May 1996)

We consider the Seebeck coefficient in  $\text{LaCrO}_3$  and related transition-metal-oxide perovskites using a model for electronic conduction based on the electronic structure of the  $3d$  orbitals of the  $B$ -site transition-metal cations. Relations for the Seebeck coefficient are presented for those perovskite systems in which electronic conduction is through the  $t_{2g}$  states of the  $B$ -site transition-metal cations. High- and low-temperature limits for the Seebeck coefficient are identified for the cases of both strong and weak magnetic coupling between electron spins. In these high- and low-temperature limits, the Seebeck coefficient is determined as a function of carrier concentration. Results are applied to an analysis of experimental data for the  $(\text{La,Sr})\text{CrO}_3$  series. [S0163-1829(96)02935-9]

**I. INTRODUCTION**

Continued interest in materials suitable for use in high-temperature electrical components has led to considerable experimental investigation<sup>1–13</sup> of a number of transition-metal oxides possessing the perovskite structure  $ABO_3$ . Many of these materials exhibit a thermally activated high-temperature electrical conductivity attributed to  $p$ -type small polarons hopping among the transition-metal  $B$ -site cations.<sup>1,2,8,14</sup> In addition to the conductivity, experimental characterization of these materials typically includes measurement of the Seebeck coefficient (or thermoelectric power) to infer values of the carrier concentration, the latter of which are then combined with measured values of the conductivity to obtain estimates of polaron mobilities. In many of the experimental thermopower studies performed to date, however, extraction of the carrier concentration from the thermoelectric power has been performed through analyses based upon temperature-independent formulas<sup>15–18</sup> for the thermopower often attributed to Heikes<sup>15,19</sup> or to Chaikin and Beni.<sup>17</sup> These formulas are certainly appropriate for the conditions under which they were developed, namely, for systems where there are one or at most two carriers of opposite spin occupying one orbital state per site. There has been some concern in recent years, however, regarding the application of these formulas to systems in which there are additional degeneracies associated with states of carrier occupation not previously considered. Doumerc,<sup>20</sup> e.g., has recently reemphasized a proper treatment of spin degeneracy for systems possessing mixed valence cations, for which he reiterates Heikes's observation<sup>15</sup> that the relevant spin (and spin degeneracy) to consider in such systems is not just that of the carriers alone, but that of the ions that they occupy. In many transition-metal-oxide perovskites there is, in addition to this spin degeneracy, more than one energetically degenerate *spatial* orbital that should similarly be considered. In  $\text{LaCrO}_3$  and  $\text{LaMnO}_3$ , e.g., the orbital degeneracy at the  $B$ -site transition-metal cations is determined by the octahe-

dral crystal field that splits the five transition-metal  $3d$  electronic orbitals into a set of lower-energy threefold-degenerate  $t_{2g}$  states and a set of doubly degenerate  $e_g$  states,<sup>14,21,22</sup> higher in energy than the  $t_{2g}$  manifold by an amount equal to the crystal field splitting parameter  $10Dq \sim 2$  eV. Thus a prerequisite to the correct extraction of carrier concentrations (and carrier mobilities) in these systems is a theory of the thermoelectric power that properly takes into account both the spin and spatial degeneracies implied by the electronic structure of the material under consideration.

In this paper theoretical expressions for the Seebeck coefficient are derived appropriate to small polaron conduction occurring among the  $3d$  transition-metal  $B$ -site manifold associated with materials of this kind. We focus in this paper on those transition-metal oxides in which electronic occupation is confined to the lower energy  $t_{2g}$  states of the  $3d$  transition-metal  $B$ -site manifold, deferring to a future paper the modifications to our theory that arise for those materials in which electronic occupation also includes the higher-energy  $e_g$  states of the transition-metal cations. Thus the analysis of the current paper should be applicable to transition-metal cations in a valence state with  $n \leq 3$  electrons in the  $3d$  manifold, such as homogeneous systems containing  $\text{Cr}^{3+}$ ,  $\text{Cr}^{4+}$ , and  $\text{Cr}^{5+}$ , or containing  $\text{V}^{2+}$ ,  $\text{V}^{3+}$ , and  $\text{V}^{4+}$  cations at the  $B$  sites. The present analysis would not be expected to apply to systems in which hopping is associated with  $\text{Mn}^{3+}$  and  $\text{Mn}^{4+}$ , or with Co cations, in which there can be unpaired electrons in both the  $t_{2g}$  and  $e_g$  levels. The different feature of the present calculation, we believe, is the manner in which the spatial and spin degeneracies associated with electronic occupation of the  $3d$  levels are explicitly treated.

The rest of the paper is laid out as follows. In Sec. II we present basic relations for the Seebeck coefficient along with a particular model of electronic conduction appropriate to transition-metal oxides of this type. In Sec. III high- and low-temperature limiting forms for the Seebeck coefficient

are derived for the cases in which magnetic coupling to neighboring cations is strong and weak, respectively. In Sec. IV we illustrate the use of these high- and low-temperature formulas in a brief analysis of existing thermopower data for the  $\text{La}_{1-x}\text{Sr}_x\text{CrO}_3$  system. Section V concludes with a brief summary.

## II. MODEL

Our goal is a calculation of the Seebeck coefficient or thermoelectric power  $S$ , operationally defined as the electrochemical potential difference per unit temperature difference that develops across an electrically isolated sample with an imposed temperature gradient. The Onsager-Casimir theory of irreversible processes<sup>23–26</sup> allows derivation of expressions that relate the Seebeck coefficient to transport quantities that are defined in the absence of a temperature gradient. Domenicali,<sup>23</sup> e.g., shows that the Seebeck coefficient can be written in the form

$$S = -\frac{k}{e} \left( \frac{Q^*}{kT} - \frac{\mu}{kT} \right), \quad (1)$$

where  $k$  is Boltzmann's constant,  $e$  the electronic charge,  $\mu$  the chemical potential,  $T$  the absolute temperature, and  $Q^*$  the ‘‘transport heat per particle,’’ defined as the ratio

$$Q^* = \left( \frac{|\mathbf{J}_q|}{|\mathbf{J}_e|} \right)_{\nabla T=0} \quad (2)$$

of energy current  $\mathbf{J}_q$  to particle current  $\mathbf{J}_e$  associated with the flow of electrons in the presence of a weak electric field and a vanishing temperature gradient. Thus  $Q^*$  can also be expressed as a ratio of transport coefficients

$$Q^* = \frac{e\xi}{\sigma}, \quad (3)$$

where  $\sigma$  is the usual isothermal electrical conductivity and  $\xi$  represents the resulting energy flow per unit of applied electric field under the same conditions. As a consequence, (1) may be expressed in the form

$$S = -\frac{k}{e} \left[ \frac{1}{kT} \left( \frac{e\xi}{\sigma} \right) - \frac{\mu}{kT} \right]. \quad (4)$$

Thus, from an appropriate microscopic Hamiltonian, the transport coefficients appearing in these expressions may be evaluated, using, e.g., linear-response theory,<sup>27,28</sup> and combined with a calculation of the chemical potential to obtain the Seebeck coefficient. We have recently adopted this strategy in developing a numerical approach for calculating the temperature dependence of the Seebeck coefficient for substitutionally mixed perovskites containing different  $B$ -site cations.<sup>29</sup> In the present paper, which is primarily concerned with the derivation of temperature-independent limiting forms for the Seebeck coefficient for homogeneous systems, we are able to employ physical arguments that allow us to avoid some of the cumbersome mathematics that is necessary in the general case.

Our starting point is a microscopic model of electron transport among the triply degenerate  $t_{2g}$  states of the  $3d$  transition-metal levels. We consider, therefore, a simplified model Hamiltonian

$$H = - \sum_{l,l',d,d'} J_{ll'}^{dd'} c_{ld}^\dagger c_{l'd'} + \epsilon_0 \sum_l n_l + \frac{1}{2} \sum_{l,d,d'} U_1^{dd'} n_{ld} n_{ld'} + \omega_0 \sum_l b_l^\dagger b_l - \lambda \omega_0 \sum_l n_l (b_l^\dagger + b_l), \quad (5)$$

which focuses on conduction electrons occupying the transition-metal  $B$  sites of the perovskite structure. In this expression,  $\epsilon_0$  is the bare energy associated with an electron occupying one of the triply degenerate  $t_{2g}$  states at site  $l$  and the operators  $c_{ld}^\dagger$ ,  $c_{ld}$ , and  $n_{ld}$  create, annihilate, and count, respectively, electrons in state  $d$  at site  $l$ , while  $n_l = \sum_d n_{ld}$  is the total number of  $d$  electrons at that site. The label  $d$  is intended to represent both orbital and spin indices associated with the  $3d$  states in the lower-energy  $t_{2g}$  manifold. The matrix element (superexchange, double exchange, etc.) for electron transitions between states  $d$  at  $B$  site  $l$  and state  $d'$  at the neighboring  $B$  site  $l'$  is  $J_{ll'}^{dd'}$ . We also include repulsive Coulomb interactions  $U_1^{dd'}$  between  $3d$  electrons at the same site. In principle, these interaction energies may be separated into three types. First there is the (Hubbard) energy  $U_0$  between electrons with opposite spin in the same  $d$  orbital. With multiple orbitals at each site, however, there is also a Coulomb energy  $U_1$  between electrons of opposite spin in different spatial orbitals. Finally, there is the Coulomb repulsion energy  $U_2$  between electrons having the same spin in different  $d$  orbitals at the same site. Hund's rules, which tend to favor configurations in which all electrons at a site have their spins aligned as much as possible, arise because interactions between electrons in different spin states are larger than those between electrons in the same spin state by an exchange energy  $\Delta_{\text{ex}} \sim U_0 - U_2 \sim U_1 - U_2$ , so that typically  $U_0 \sim U_1 \gg U_2$ . In what follows we assume that  $kT \ll U_0 \sim U_1$ , so that any site configurations of interest only involve electrons with the same spin orientation. By precluding other configurations and processes, therefore, we can ignore the energies  $U_0$  and  $U_1$  and take as our main focus an understanding of the role played by the Coulomb energy  $U_2 \equiv U$  associated with electrons in different spatial orbitals at the same site. We do not explicitly include in our Hamiltonian interactions between electrons on neighboring sites, i.e., terms that could lead to a collective ferromagnetic or antiferromagnetic alignment of the spins. These exchange terms have previously been treated for a single-orbital model within mean-field theory.<sup>30</sup> In the multiple-orbital model considered in the present paper, a self-consistent treatment becomes complicated by the increased number and type of such interactions. Of course, the magnitude of interatomic Coulomb interactions, which involve integrals associated with orbitals on different sites, are generally expected to be smaller in magnitude than corresponding interactions associated with electrons on the same cation. It is difficult, however, to compare *a priori* the interaction energy associated with electrons of opposite spin on neighboring sites to that associated with electrons of the same spin at the same site. In

what follows we take a simple approach that phenomenologically treats exchange interactions between electrons on neighboring sites through a modification of the relevant spin degeneracies at each site. This restriction of the spin degeneracies is discussed more fully in Sec. III.

In keeping with the polaronic nature of conduction in these materials, we have also included in our Hamiltonian (5) a coupling to a narrow band of optical phonons. In the last two terms, therefore,  $b_l^\dagger$  and  $b_l$  create and annihilate, respectively, vibrational excitations of the lattice at site  $l$ . The strength of the coupling term (linear in the oscillator displacements) is governed by the electron-phonon coupling constant  $\lambda$  and the total number of  $3d$  electrons at a site. This electron-phonon part of the Hamiltonian can be diagonalized by a well-known unitary transformation<sup>31-33</sup>  $u = \exp[\lambda \sum_l n_l (b_l - b_l^\dagger)]$ , that preserves fermion number operators and commutation relations and gives rise to ‘‘displaced’’ phonon operators  $\tilde{b}_l = b_l - \lambda n_l$  and ‘‘dressed’’ electron operators  $\tilde{c}_{ld} = c_{ld} \exp[\lambda n_l (b_l - b_l^\dagger)]$  describing the polarons. The total Hamiltonian, when expressed in terms of the new set of operators, takes the form

$$H = - \sum_{l,l',d,d'} \tilde{J}_{ll'}^{dd'} \tilde{c}_{ld}^\dagger \tilde{c}_{l'd'} + \tilde{\epsilon}_0 \sum_l n_l + \frac{1}{2} \sum_{l,d,d'} \tilde{U}^{dd'} n_{ld} n_{ld'} + \omega_0 \sum_l \tilde{b}_l^\dagger \tilde{b}_l, \quad (6)$$

in which the dressed matrix element  $\tilde{J}_{ll'}^{dd'} = J_{ll'}^{dd'} \exp[\lambda(b_l - b_l^\dagger - b_{l'} + b_{l'}^\dagger)]$  is now a function of the new phonon operators, while the renormalized site energies  $\tilde{\epsilon}_0 = \epsilon_0 - \lambda^2 \omega_0$  and interaction energies  $\tilde{U}_l^{dd'} = U_l^{dd'} - \lambda^2 \omega_0$  are reduced from their bare values due to the interaction with the lattice. In what follows, we work in the localized site basis, assuming that the mean value of the transfer term  $\langle \tilde{J}_{ll'}^{dd'} \rangle$  is small, an assumption that is, again, in keeping with the polaronic nature of transport in these materials.

The transport coefficients  $\sigma$  and  $\xi$  required for evaluating the Seebeck coefficient characterize charge and energy flow in the presence of a weak electric field. In order to obtain expressions for these, we begin with a microscopic version of the continuity equation for charge flow

$$e \frac{\partial n_l}{\partial t} = \sum_{l'} (j_{ll'} - j_{l'l}). \quad (7)$$

Using the Heisenberg relation  $i \partial n_l / \partial t = [n_l, H]$  along with the Hamiltonian (6), it is straightforward to obtain an expression for the operator representing the microscopic charge current

$$j_{ll'} = -i \sum_{d,d'} e (\tilde{J}_{ll'}^{dd'} \tilde{c}_{ld}^\dagger \tilde{c}_{l'd'} - \tilde{J}_{l'l}^{d'd} \tilde{c}_{l'd'}^\dagger \tilde{c}_{ld}), \quad (8)$$

which flows between a typical site  $l$  and its neighbor at  $l'$ . A calculation of the operator describing energy flow proceeds in an analogous fashion. First, we express the total Hamiltonian (6) as a sum  $H = \sum_l H_l$  of local terms

$$H_l = - \sum_{l',d,d'} (\tilde{J}_{ll'}^{dd'} \tilde{c}_{ld}^\dagger \tilde{c}_{l'd'} + \tilde{J}_{l'l}^{d'd} \tilde{c}_{l'd'}^\dagger \tilde{c}_{ld}) + \frac{1}{2} \sum_{d,d'} \tilde{U}_l^{dd'} n_{ld} n_{ld'} + \tilde{\epsilon}_0 \sum_d n_{ld} + \omega_0 \tilde{b}_l^\dagger \tilde{b}_l, \quad (9)$$

each representing the energy associated with a single site. Conservation of energy then leads, as in the case of particle number, to a microscopic continuity equation

$$\frac{\partial H_l}{\partial t} = \sum_{l'} (q_{ll'} - q_{l'l}) \quad (10)$$

involving energy flow. Using the Heisenberg equations of motion for the operators  $H_l$ , we obtain an expression for the energy current operator

$$q_{ll'} = i \sum_{d,d'} \tilde{\epsilon}_0 (\tilde{J}_{ll'}^{dd'} \tilde{c}_{ld}^\dagger \tilde{c}_{l'd'} - \tilde{J}_{l'l}^{d'd} \tilde{c}_{l'd'}^\dagger \tilde{c}_{ld}) + i \sum_{d,d',d''} \tilde{U}_l^{dd''} n_{ld''} (\tilde{J}_{ll'}^{dd'} \tilde{c}_{ld}^\dagger \tilde{c}_{l'd'} - \tilde{J}_{l'l}^{d'd} \tilde{c}_{l'd'}^\dagger \tilde{c}_{ld}) = q_{ll'}^\epsilon + q_{ll'}^U. \quad (11)$$

In the last line we have implicitly separated the energy current into two terms, the first corresponding to the flow  $q_{ll'}^\epsilon$  of site energy and the second to the flow  $q_{ll'}^U$  of interaction energy, and neglected a term associated with the flow of kinetic energy, which is of second order in the polaron bandwidth.

We now note that the three operators  $j_{ll'}$ ,  $q_{ll'}^\epsilon$ , and  $q_{ll'}^U$  are nearly identical in form, in that they all appear as sums over the different transfer events that can occur, weighted by that which is transferred for each event. For example, the term  $e \tilde{J}_{ll'}^{dd'} \tilde{c}_{ld}^\dagger \tilde{c}_{l'd'}$  appearing in the charge current operator corresponds to the transition of an electron from state  $d'$  at site  $l'$  to a state  $d$  at site  $l$ , which carries with it charge  $e$ . Similarly, the term  $\tilde{\epsilon}_0 \tilde{J}_{ll'}^{dd'} \tilde{c}_{ld}^\dagger \tilde{c}_{l'd'}$  appearing in the energy current operator represents the same type of event, but describes one unit of site energy  $\tilde{\epsilon}_0$  being carried to site  $l$ . The term  $(\sum_{d''} \tilde{U}_l^{dd''} n_{ld''}) \tilde{J}_{ll'}^{dd'} \tilde{c}_{ld}^\dagger \tilde{c}_{l'd'}$  in (11) represents again the same event, but characterizes the increase at site  $l$  of the interaction energy, a quantity that depends upon the population of electrons already at that site. It is reasonable, in view of this similarity of structure, to expect the particle current and energy current associated with such events to be, on average, proportional to one another. In what follows we explore this idea further for specific parameter regimes.

### III. LIMITING FORMS

In keeping with the picture that we have developed, we focus on the situation where the average number  $\rho = \langle n_l \rangle$  of  $3d$  electrons per site (which in general will depend upon the  $A$ -site doping level) is restricted to lie in the range  $3 \geq \rho \geq 0$ . This, along with our assumption that  $kT \ll U_0 \sim U_1$ , allows us to ignore any configurations with electrons of opposite spin at the same site. Even with this

restriction, to properly account for the degeneracy of a given configuration, we note that the total spin associated with  $n$  electrons with the same spin alignment is

$$\sigma = ns = \frac{n}{2}. \quad (12)$$

If the coupling between spins on neighboring cations is sufficiently weak (or the temperature sufficiently high), then there will be a maximum spin degeneracy

$$\Gamma_n^\sigma = 2\sigma + 1 = n + 1 \quad (13)$$

associated with a weakly coupled site configuration having  $n$  aligned electrons. In many transition-metal oxides, however, there is significant ferromagnetic or antiferromagnetic coupling between cation spins at neighboring sites, so that at sufficiently low temperatures the spin orientation at a given site is fixed relative to that of its neighbors. In this strong-coupling limit, therefore, the effective spin degeneracies  $\gamma_\sigma$  of each electron, and  $\Gamma_n^\sigma$  of the configuration as a whole, are reduced to unity, i.e.,  $\Gamma_n^\sigma = 1$ , since there is only one energetically favorable spin state associated with the electrons in that configuration. In what follows we explicitly consider both limiting cases, which we will refer to as the limit of weak and strong magnetic coupling, respectively.

#### A. Temperatures large compared to the Coulomb energies

We consider first the high-temperature limit in which the thermal energy  $kT$  is much greater than the Coulomb energy  $U$  between electrons in different  $t_{2g}$  orbitals at the same site, i.e.,  $kT \gg U$ . We will see that, in this limit, the Seebeck coefficient is dominated by contributions from the chemical potential. Physically, this occurs because the energy carried per particle is bounded by an amount on the order of  $U$ , so that the ratio  $\xi/\sigma$  appearing in (4) approaches a constant, while the chemical potential grows with temperature, eventually dominating the energy current.

To see this in more detail, we break the coefficient  $\xi = \xi^\epsilon + \xi^U$  into two parts, the first  $\xi^\epsilon$  describing the flow of site energy  $q_{ll'}^\epsilon$ , and the second  $\xi^U$  describing the flow of interaction energy  $q_{ll'}^U$ . [From this point on, in the interest of notational simplicity, we drop all tildes with the understanding that symbols refer to the dressed quantities appearing in Eq. (6).] From (11) it is clear that, with the site energy of all  $t_{2g}$  orbitals the same, we can write  $\xi^\epsilon = \epsilon_0 \sigma / e$ , so that there is a fixed amount of site energy per charge carried along by the particle current. Such a strict proportionality does not occur for the interaction energy operator  $q_{ll'}^U$ , in (11), but it is clear that there is a maximum amount of interaction energy  $\bar{U}$  that will be carried per charge. In this problem, the maximum interaction energy is transferred, e.g., when an electron hops onto a neighboring site in which there are electrons already occupying two of the three degenerate  $t_{2g}$  orbitals at that site. Thus there exists an energy  $\bar{U} \sim U$  for which we can write  $\langle q_{ll'}^U \rangle \leq (\bar{U}/e) \langle j_{ll'} \rangle$ , so that, quite generally,

$$\xi^U \leq \frac{\bar{U}}{e} \sigma. \quad (14)$$

Thus the quantity appearing in (4) for the Seebeck coefficient separates into two terms

$$\frac{1}{kT} \left( \frac{e\xi}{\sigma} \right) = \frac{e(\xi^U + \xi^\epsilon)}{\sigma kT} \sim \frac{\bar{U}}{kT} + \frac{\epsilon_0}{kT} \sim \frac{\epsilon_0}{kT}, \quad (15)$$

where in the last step we have neglected the term  $\bar{U}/kT$ , which is assumed to be small in the limit of interest. The second term in (15) involving the site energy, it turns out, will exactly cancel an equal and opposite term obtained from the chemical potential. We therefore make no assumption at this point about the magnitude of this second term, which also decreases with increasing temperature, but may or may not remain large.

Having established the high-temperature limiting form for the ratio of transport coefficients (15), it remains to evaluate the chemical potential in order to produce a corresponding limiting expression for the Seebeck coefficient. In keeping with the physics of the problem, it suffices to evaluate the chemical potential to lowest (i.e., zeroth order) in the transfer matrix element  $\tilde{J}_{ll'}^{dd'}$ , whose expectation value  $\langle \tilde{J}_{ll'}^{dd'} \rangle$  is that of the greatly reduced polaron bandwidth. Neglect of the transfer term in (6) decouples the phonon and polaron subsystems and also decouples from one another the electrons at different sites. We proceed, therefore, by calculating the grand partition function

$$Q = \text{Tr} \{ e^{-\beta(H_I - \mu n_l)} \} \quad (16)$$

for the electrons at each site, where the decoupled site Hamiltonian

$$H_I = \epsilon_0 n_l + \frac{1}{2} \sum_{d,d'} U n_{ld} n_{ld'} \quad (17)$$

is the same for each site in the system and the trace in (16) is only over configurations with aligned electrons. In the high-temperature limit of interest, exponentials of  $U/kT$  approach unity and each term in the partition function is largely determined by those parts of the exponential involving the chemical potential  $\mu$  and the site energy  $\epsilon_0$ . Taking spin degeneracy into account we find that

$$Q = \sum_{n=0}^3 \frac{3! \Gamma_n^\sigma}{(3-n)! n!} e^{n\beta(\mu - \epsilon_0)}, \quad (18)$$

where the combinatorial factor gives the number of distinct configurations in which there are carriers occupying  $n$  of the 3 distinct single-particle states available at this site and, in keeping with our previous discussion, the spin degeneracy

$$\Gamma_n^\sigma = \begin{cases} n+1 & \text{for weak magnetic coupling} \\ 1 & \text{for strong magnetic coupling} \end{cases} \quad (19)$$

is that of a configuration of  $n$  aligned electrons, the form of which we take to depend, in a simple way, upon the strength of exchange interactions between electron spins on nearest-neighbor lattice sites (terms, as we have noted, that have been left out of the Hamiltonian). As suggested in (18), we separately treat the two limiting cases in which nearest-neighbor interactions are small compared to thermal energies

(weak magnetic coupling) and large compared to thermal energies (strong magnetic coupling).

We consider first the case of strong magnetic coupling, for which  $\Gamma_n^\sigma = 1$  and for which the sum (18) can be identified as the binomial expansion of

$$Q = [1 + e^{\beta(\mu - \epsilon_0)}]^3. \quad (20)$$

The average number of  $3d$  electrons per site  $\rho$ , as a function of the chemical potential and temperature, can then be obtained in this limit from the site partition function through the relation

$$\rho = \frac{1}{\beta Q} \frac{\partial Q}{\partial \mu} = \frac{3}{1 + e^{-\beta(\mu - \epsilon_0)}}, \quad (21)$$

which is simply the total number of degenerate orbitals per site multiplied by the Fermi-Dirac distribution function for degenerate states of energy  $\epsilon_0$ . Inverting Eq. (21) yields an expression for the chemical potential

$$\frac{\mu}{kT} = \frac{\epsilon_0}{kT} - \ln \left[ \frac{3 - \rho}{\rho} \right]. \quad (22)$$

Combining this with (15), we find that for strong magnetic coupling and  $kT \gg U$ , the Seebeck coefficient can be written

$$S = -\frac{k}{e} \ln \left( \frac{3 - \rho}{\rho} \right). \quad (23)$$

For the case of weak magnetic coupling the spin degeneracy  $\Gamma_n^\sigma = n + 1$  takes its maximum value, and although the resulting sum for the partition function

$$Q = \sum_{n=0}^3 \frac{3!(n+1)}{(3-n)!n!} e^{n\beta(\mu - \epsilon_0)} \quad (24)$$

is no longer a simple binomial expansion, it is still readily evaluated, i.e.,

$$Q = [1 + e^{\beta(\mu - \epsilon_0)}]^2 [1 + 4e^{\beta(\mu - \epsilon_0)}]. \quad (25)$$

This leads then to an expression for the average  $3d$  electron site concentration

$$\rho = \frac{1}{\beta Q} \frac{\partial Q}{\partial \mu} = \frac{3e^{\beta(\mu - \epsilon_0)} [2 + 4e^{\beta(\mu - \epsilon_0)}]}{[1 + e^{\beta(\mu - \epsilon_0)}][1 + 4e^{\beta(\mu - \epsilon_0)}]}. \quad (26)$$

Multiplying through by the denominator gives a quadratic equation for  $e^{\beta\mu}$  as a function of  $\rho$ . Keeping the physical root, we obtain an expression for the chemical potential as a function of  $\rho$ , which, when combined with (15) in (4), results in an expression for the Seebeck coefficient

$$S = -\frac{k}{e} \ln \frac{8(3 - \rho)}{(5\rho - 6) - \sqrt{36 - 12\rho + 9\rho^2}} \quad (27)$$

valid for weak magnetic coupling and  $kT \gg U$ .

Equations (23) and (27) derived for the high-temperature Seebeck coefficient for strong and weak magnetic coupling can also be expressed in terms of the hole concentration  $\rho_h$ , a quantity that is more directly related to the level of acceptor doping. The number  $\rho_0$  of  $3d$  electrons per site in the end member of a particular compositional series will de-

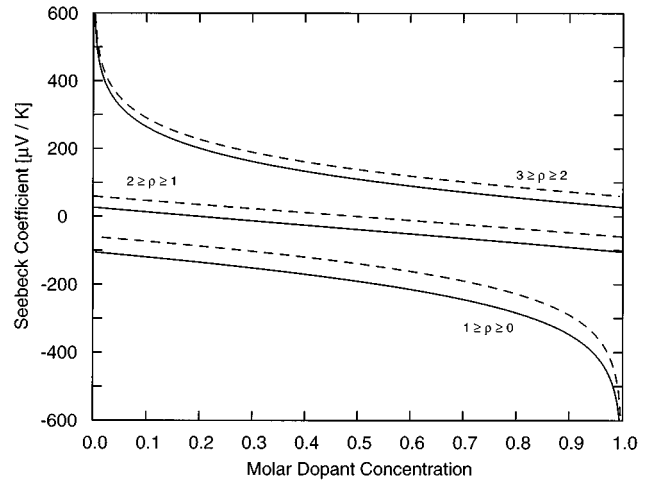


FIG. 1. High-temperature limit of the Seebeck coefficient as a function of the molar dopant concentration for the case of  $3d$  transition-metal  $t_{2g}$  occupation. Three systems are shown in which the undoped end member electronic occupation  $\rho_0$  takes the values of 1, 2, and 3, representing, e.g.,  $\text{Ti}^{3+}$ ,  $\text{V}^{3+}$ , and  $\text{Cr}^{3+}$  cations at the  $B$  sites, respectively. The solid lines and dashed lines represent the limits of weak and strong magnetic coupling between neighboring sites. The lower curves correspond to  $\rho_0 = 1$ , with  $1 \geq \rho \geq 0$ , the middle curves to  $\rho_0 = 2$ , with  $2 \geq \rho \geq 1$ , and the upper curves to  $\rho_0 = 3$ , with  $3 \geq \rho \geq 2$ .

pend upon the particular species of  $A$ - and  $B$ -site cation associated with the material. In transition-metal lanthanides, such as  $\text{LaMnO}_3$  and  $\text{LaCrO}_3$ , e.g., the  $B$ -site transition-metal cations are in a trivalent state. Under these circumstances, substitution of divalent cations such as  $\text{Sr}^{2+}$  at the  $A$  site removes electrons at the  $B$  sites to change the average  $3d$  electronic site concentration  $\rho$  by creating holes<sup>34</sup> in site concentration  $\rho_h = \rho_0 - \rho$ . Thus we can rewrite (23) and (27) in terms of the hole concentration  $\rho_h$  and the expected electronic site concentration  $\rho_0$  of the end member. After this substitution the strong-coupling result (23) takes the form

$$S = -\frac{k}{e} \ln \left( \frac{3 - \rho_0 + \rho_h}{\rho_0 - \rho_h} \right), \quad (28)$$

while the weak-coupling result can be written

$$S = -\frac{k}{e} \ln \frac{8(3 - \rho_0 + \rho_h)}{5(\rho_0 - \rho_h) - 6 - \sqrt{36 - 12(\rho_0 - \rho_h) + 9(\rho_0 - \rho_h)^2}}. \quad (29)$$

In Fig. 1 we plot values of the Seebeck coefficient predicted by Eqs. (28) and (29) for compositional series in which the initial (undoped) stoichiometric electronic occupation of the end member takes three different values  $\rho_0 = 1, 2$ , and  $3$ , representing, respectively,  $\text{Ti}^{3+}$ ,  $\text{V}^{3+}$ , and  $\text{Cr}^{3+}$  cations in a perovskite with a nominally trivalent  $A$ -site end member. In these curves the high-temperature Seebeck coefficient for strong and weak magnetic coupling is shown as a function of the dopant concentration, assumed to be equal to the hole site concentration  $\rho_h = \rho_0 - \rho$ . The strong-coupling results are presented as solid lines and the weak-coupling results as dashed lines. We note that the effect of orbital degeneracy is very large, in that the Seebeck coefficient for

two series having the same number of ‘‘holes’’ depends very strongly on the number of available hole states per site and therefore on the particular electronic configuration of the  $B$ -site cation.

### B. Temperatures low compared to the Coulomb energies

We now consider the opposite limit  $kT \ll U$  in which thermal energies are small compared to the Coulomb energy between electrons in different  $t_{2g}$  orbitals at the same site. We note first that in this limit electrons will avoid piling up on the same site as much as possible in order to avoid the energy cost  $U$  associated with having multiple electrons at the same site. Thus all sites will first fill up to the same number  $n_0 \leq 2$  of electrons per site, leaving some excess average site population  $\rho_e = \rho - n_0 \leq 1$ , which will be distributed with at most one excess electron at any given lattice site. States will, of course, fill up according to Hund’s rules, so that for  $\rho < 3$  any excess electron will go into a state aligned with that of the  $3d$  electrons already at that site (if any). Under these circumstances, the probability of any process that would transfer an excess electron to a site already containing an excess electron will be weighted by an exponentially small Boltzmann factor of the form  $e^{-\beta U}$  relative to those processes in which the transfer takes place to a site with the minimum filled electron population  $n_0$ . Similar arguments would preclude transfers of an electron out of a site containing the minimum number  $n_0$  of filled electrons onto a site already containing the minimum number.

In the low-temperature limit, therefore, the flow of particle and energy current is completely dominated by processes involving the transfer of an excess electron between two sites that otherwise would be populated by  $n_0$  electrons. The energy at the site to which the particle hops will then be larger than it was before the hop occurred by an amount equal to  $\epsilon_0 + n_0 U$ , the first term being the site energy, the second being associated with the interaction energy current. This argument leads to the conclusion that, at low temperatures, the energy current must be strictly proportional to the particle current and in particular that

$$\xi = (\epsilon_0 + n_0 U) \frac{\sigma}{e}. \quad (30)$$

Thus, in this limit

$$\frac{1}{kT} \left( \frac{e\xi}{\sigma} \right) = \frac{\epsilon_0 + n_0 U}{kT} = \frac{\epsilon_0 + \tilde{U}}{kT}, \quad (31)$$

where we have introduced  $\tilde{U} = n_0 U_0$  as the interaction energy carried by the electronic transition in this limit. In evaluating the chemical potential  $\mu$  for large Coulomb energies and low temperatures we again neglect all contributions to the site partition function (16) from configurations with unaligned electrons and obtain the result

$$Q = e^{-\beta n_0 [\epsilon_0 - \mu - (1/2)(n_0 - 1)U]} [\beta_0 + \beta_1 e^{-\beta(\epsilon_0 + \tilde{U} - \mu)}], \quad (32)$$

which is essentially a sum of two terms. The first term inside the square brackets is associated with site configurations having the minimum electronic occupation  $n_0$  and is associated with a degeneracy

$$\beta_0 = \frac{3! \Gamma_0^\sigma}{(3 - n_0)! n_0!} = \Gamma_0 \Gamma_0^\sigma, \quad (33)$$

which is a product of the orbital degeneracy  $\Gamma_0 = 3!/(3 - n_0)! n_0!$  and the spin degeneracy  $\Gamma_0^\sigma$ , which depends upon the magnetic coupling as in (19), i.e.,

$$\Gamma_0^\sigma = \begin{cases} n_0 + 1 & \text{for weak magnetic coupling} \\ 1 & \text{for strong magnetic coupling.} \end{cases} \quad (34)$$

The second term in square brackets in (32) is associated with configurations having  $n_0 + 1$  electrons or one excess electron. The degeneracy  $\beta_1 = \Gamma_1 \Gamma_1^\sigma$  of such configurations is that obtained by replacing  $n_0$  by  $n_0 + 1$  in (33) and (34). We can develop an expression that is correct for both weak- and strong-coupling limits by formally taking derivatives of (32) to obtain the electron density  $\rho$ , as in (21). Inverting the resulting expression then yields the chemical potential

$$\mu = \epsilon_0 + \tilde{U} + kT \ln \left[ \frac{\beta_0}{\beta_1} \left( \frac{\rho_e}{1 - \rho_e} \right) \right], \quad (35)$$

which can be substituted along with (31) into (4). When this is done the terms involving the ratio  $(\epsilon_0 + \tilde{U})/kT$  cancel exactly, leaving the following expression for the low-temperature Seebeck coefficient:

$$S = -\frac{k}{e} \ln \left[ \frac{\beta_1}{\beta_0} \left( \frac{1 - \rho_e}{\rho_e} \right) \right], \quad (36)$$

valid in the limit  $U \gg kT$ . The excess fractional electron population  $\rho_e$  in this expression has values lying between zero and one. It is interesting to note that in this limit we recover a form identical to that obtained earlier by Doumerc,<sup>20</sup> except for an implicit extension to include both orbital and spin degeneracy.

As in the high-temperature limit, it is useful to represent the Seebeck coefficient in terms of the average hole population  $\rho_h$ , which in the present low-temperature limit is equivalent to the fraction of sites having the *minimum* filled electronic occupation  $n_0$  and is related to the excess electronic population  $\rho_e$  through the relation  $\rho_h = 1 - \rho_e$ . Thus (36) can also be expressed in the form

$$S = \frac{k}{e} \ln \left[ \frac{\beta_0}{\beta_1} \left( \frac{1 - \rho_h}{\rho_h} \right) \right]. \quad (37)$$

We now develop special cases of this expression appropriate to both strong and weak magnetic coupling.

In the limit of strong magnetic coupling, the spin degeneracies are equal to unity, i.e.,  $\Gamma_0^\sigma = \Gamma_1^\sigma = 1$ , so that  $\beta_0 = \Gamma_0 = 3!/(3 - n_0)! n_0!$  and  $\beta_1 = \Gamma_1 = 3!/(3 - n_0 - 1)!(n_0 + 1)!$ . Thus, for strong magnetic coupling and low temperatures, (37) can be written

$$S = \frac{k}{e} \ln \left[ \frac{\rho_0}{4 - \rho_0} \left( \frac{1 - \rho_h}{\rho_h} \right) \right], \quad (38)$$

where, as before,  $\rho_0 = n_0 + 1$  represents the undoped  $3d$  site population of the end member of the series to be acceptor doped and  $\rho_h = \rho_0 - \rho$  is the fraction of holes that have been introduced as a result of acceptor doping.

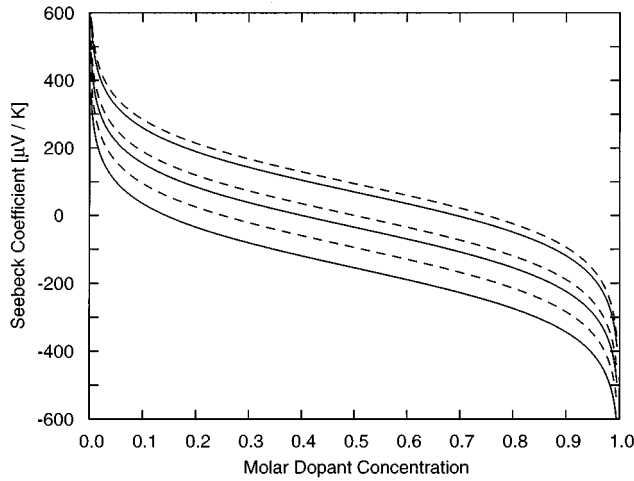


FIG. 2. Seebeck coefficient shown as a function of the molar dopant concentration for the limiting case where  $kT \ll U$ . Systems are shown in which the undoped end member electronic occupation number  $\rho_0$  takes the values 1, 2, and 3, representing, e.g.,  $\text{Ti}^{3+}$ ,  $\text{V}^{3+}$ , and  $\text{Cr}^{3+}$  cations at the  $B$  sites, respectively. The solid lines and dashed lines represent the limits of weak and strong magnetic coupling between neighboring sites. The lower curves correspond to  $\rho_0=1$ , with  $1 \geq \rho \geq 0$ , the middle curves to  $\rho_0=2$ , with  $2 \geq \rho \geq 1$ , and the upper curves to  $\rho_0=3$ , with  $3 \geq \rho \geq 2$ .

In the limit of weak magnetic coupling the spin degeneracies  $\Gamma_0$  and  $\Gamma_1$  have their maximum values of  $n_0+1$  and  $n_0+2$ , respectively. In this limit, of course, we are implicitly assuming a significant separation in the scale of electron interactions at the same site  $U_{II}$  relative to interactions  $U_{II'}$  associated with electrons at neighboring sites, so that  $U_{II} \gg kT \gg U_{II'}$ . In  $\text{LaCrO}_3$ , for example, intersite exchange interactions occur through overlap between the cation  $t_{2g}$  orbitals and the oxygen  $p$  orbitals. The strength of this interaction in  $\text{LaCrO}_3$  has been estimated by Goodenough<sup>14</sup> to be less than 300 K. Substituting in the maximum spin degeneracy, we obtain

$$\frac{\beta_0}{\beta_1} = \frac{(n_0+1)^2}{(3-n_0)(n_0+2)}, \quad (39)$$

so that for weak magnetic coupling our general low-temperature expression (37) for the Seebeck coefficient takes the form

$$S = \frac{k}{e} \ln \left[ \frac{\rho_0^2}{(4-\rho_0)(\rho_0+1)} \left( \frac{1-\rho_h}{\rho_h} \right) \right]. \quad (40)$$

In Fig. 2 we show results that represent the low-temperature counterpart to those presented in Fig. 1. As we have noted, in those systems where conduction takes place through the  $3d$  transition-metal  $t_{2g}$  states of  $B$ -site cations in a perovskite oxide, the stoichiometric electronic occupation  $\rho_0$  of the end member will depend upon the particular composition of the material. Cases are shown for which the initial stoichiometric electronic occupation of the undoped end member takes the same three values,  $\rho_0=1, 2$ , and  $3$ , as those appearing in Fig. 1. Calculations associated with weak magnetic coupling are presented as solid lines, while those associated with strong magnetic coupling are presented as

TABLE I. Electronic configurations of  $B$ -site cations for specific electronic occupation of the  $t_{2g}$  states. For each case the orbital degeneracy  $\Gamma_n$  and the spin degeneracy  $\Gamma_n^\sigma$  allowed by Hund's rules in the weak-coupling limit are shown. For strong magnetic coupling there is no spin degeneracy. Also included is the total degeneracy  $\beta_n$  of each configuration for the limits of strong and weak magnetic coupling between neighboring cations.

$t_{2g\uparrow}^n$	$\Gamma_n$	$\Gamma_n^\sigma$ (weak)	$\beta_n$ (weak)	$\beta_n$ (strong)
$t_{2g\uparrow}^0$	1	1	1	1
$t_{2g\uparrow}^1$	3	2	6	3
$t_{2g\uparrow}^2$	3	3	9	3
$t_{2g\uparrow}^3$	1	4	4	1

dashed lines. A careful inspection of Fig. 2 reveals that each of the curves in this figure can be generated through a simple vertical shift from a single curve. Using basic properties of the logarithm, it is possible to separate our basic low-temperature result (37) into two parts

$$S = \frac{k}{e} \ln \left( \frac{1-\rho_h}{\rho_h} \right) + \Delta S_d, \quad (41)$$

where the first part depends entirely upon the hole concentration and is equivalent to Heikes's formula, while the second part represents the shift observed in Fig. 2. This shift can be written

$$\Delta S_d = \ln \left( \frac{\beta_0}{\beta_1} \right) = \frac{k}{e} \ln \left( \frac{\Gamma_0}{\Gamma_1} \right) + \frac{k}{e} \ln \left( \frac{\Gamma_0^\sigma}{\Gamma_1^\sigma} \right) = \Delta S_d^\sigma + \Delta S_d^o \quad (42)$$

as a sum of two terms that contain information about the spin and orbital degeneracy of the system. In Table I possible configurations  $t_{2g\uparrow}^n$  of the  $3d$  transition-metal orbitals are shown for electronic occupation  $n=1, 2$ , and  $3$ , along with the spatial degeneracies  $\Gamma_n$ , the spin degeneracies  $\Gamma_n^\sigma = n+1$  associated with the weak-coupling limit, and the total degeneracies  $\beta_n = \Gamma_n \times \Gamma_n^\sigma$  associated with those configurations, in both the weak- and strong-magnetic-coupling limits. In Table II the information from Table I is used to compute the shift (42) in the low-temperature Seebeck coefficient, relative to Heikes's formula, for systems with electron-hole configurations of the form  $\{t_{2g\uparrow}^{n+1}, t_{2g\uparrow}^n\}$  as shown, for  $B$ -site cations in which these configurations correspond to valence states of the form  $\{M^{3+}, M^{4+}\}$ , along with the shifts in the Seebeck coefficient due to the degeneracy of each configuration for the limits of strong and weak magnetic coupling.

TABLE II. Shift in the Seebeck coefficient relative to Heikes's formula in the strong- and weak-magnetic-coupling limits for the specific electron-hole configurations shown. In the strong-coupling limit  $\Delta S_d^\sigma = 0$ .

Configuration [electron, hole]	Strong $\Delta S_d^o$ ( $\mu\text{V/K}$ )	Weak $\Delta S_d^o + \Delta S_d^\sigma$ ( $\mu\text{V/K}$ )
$[t_{2g\uparrow}^1, t_{2g\uparrow}^0]$	-94.7	-154.4
$[t_{2g\uparrow}^2, t_{2g\uparrow}^1]$	0.0	-34.9
$[t_{2g\uparrow}^3, t_{2g\uparrow}^2]$	94.7	69.9

#### IV. APPLICATION TO THE $\text{La}_{1-x}\text{Sr}_x\text{CrO}_3$ SYSTEM

We conclude by demonstrating how expressions for the Seebeck coefficient developed in this paper can be used to explain existing Seebeck coefficient data for the perovskite series  $\text{La}_{1-x}\text{Sr}_x\text{CrO}_3$ . The undoped end member of the  $\text{La}_{1-x}\text{Sr}_x\text{CrO}_3$  system,  $\text{LaCrO}_3$  has  $\rho_0 = 3$  aligned electrons filling the  $t_{2g}$  transition-metal orbitals. Divalent Sr cations substituted at the  $A$  site for trivalent La cations act as an acceptor dopant, changing the carrier concentration according to the Verwey principle.<sup>34</sup> We assume that, in spite of the mixed cation nature of the  $A$  site in this series, it can still be treated as a homogeneous system since all  $B$  sites in the sample are occupied by Cr cations and thus the set of available electronic states at each site are, to lowest order, the same.

Our results of the preceding section indicate that the magnitude of the Seebeck coefficient as a function of the dopant-hole concentration  $\rho_h = \rho_0 - \rho$  depends upon the temperature and the strength of the coupling of the spins on a given cation to those of its neighbors. Specifically, we found that in the *low-temperature* limit the Seebeck coefficient for this system can be written from (38) in the form

$$S = \frac{k}{e} \ln \left[ \frac{3}{1} \left( \frac{1 - \rho_h}{\rho_h} \right) \right] \quad (43)$$

if there is strong magnetic coupling between neighboring spins and from (40) in the form

$$S = \frac{k}{e} \ln \left[ \frac{9}{4} \left( \frac{1 - \rho_h}{\rho_h} \right) \right] \quad (44)$$

if there is weak coupling between neighboring spins.

Similarly, we found that in the *high-temperature* limit, for strong magnetic coupling, the Seebeck coefficient can be written from Eq. (23) in the form

$$S = \frac{k}{e} \ln \left( \frac{3 - \rho_h}{\rho_h} \right), \quad (45)$$

where  $\rho_h = 3 - \rho$ . Finally, in the limit of weak magnetic coupling and high temperatures, (27) for the Seebeck coefficient reduces with  $\rho = 3 - \rho_h$  to the form

$$S = \frac{k}{e} \ln \frac{9 - 5\rho_h - \sqrt{9\rho_h^2 - 42\rho_h + 81}}{8\rho_h}. \quad (46)$$

In Fig. 3 we plot values of the high- and low-temperature Seebeck coefficient as a function of  $A$ -site substitution for both limits of weak and strong magnetic coupling, as predicted by Eqs. (43)–(46). These curves, which were produced with no adjustable parameters, are compared with experimental Seebeck coefficient data for the  $\text{La}_{1-x}\text{Sr}_x\text{CrO}_3$  series from the study of Karim and Aldred<sup>8</sup> at both the low (400 K) and the high (1400 K) range of temperatures for which they obtained data. The basic trend observed in the data, with an increased spreading between the high- and low-temperature limits at higher doping levels, is clearly captured by both sets of theoretical curves. Of the two, those curves corresponding to *weak magnetic coupling* appear to most closely match the experimental results. This seems to be consistent with magnetic susceptibility measurements in the

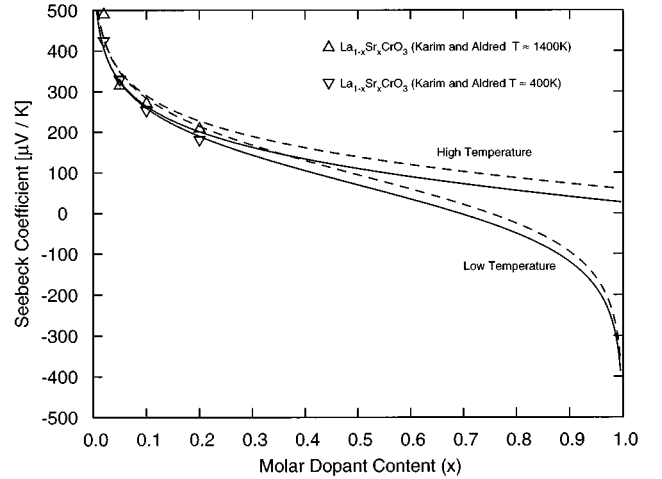


FIG. 3. Predicted high- and low-temperature limits of the Seebeck coefficient as a function of acceptor doping calculated for the  $\text{La}_{1-x}\text{Sr}_x\text{CrO}_3$  series. Experimental data are from the study of Karim and Aldred (Ref. 8) for  $\text{La}_{1-x}\text{Sr}_x\text{CrO}_3$  at high and low temperatures as indicated. Solid lines indicate predictions for weak magnetic coupling, dashed lines for strong magnetic coupling.

study of Bansal *et al.*<sup>35</sup> and Song *et al.*<sup>36</sup> which indicate that although  $\text{La}_{1-x}\text{Sr}_x\text{CrO}_3$  is antiferromagnetic at low temperatures, the ordering transition occurs at approximately 300 K. Our analysis, as indicated in Fig. 3, suggests that even by 400 K the thermal destruction of short-range order is sufficient to substantially increase the effective degeneracy seen by electrons on the  $B$  sites of this material. It is also interesting to note that our theoretical results provide a simple explanation for the relative temperature independence of the Seebeck coefficient observed in the materials of this series. At the simplest level, the small temperature dependence observed reflects a similarly small difference in the high- and low-temperature limits resulting from our analysis (see, e.g., Fig. 3). Our theory would predict a larger variation of the Seebeck coefficient with temperature at large doping levels where a considerable difference is predicted between the high- and low-temperature limits. In our analysis, this small predicted difference results from the severe constraints that are placed upon allowed configurations by the relatively low doping levels. In these systems, the hole concentration limits the maximum number of sites in the system that can exist in other than trivalent states. Thus, e.g., even though at high temperatures there is sufficient energy to create pentavalent Cr cations, this would require bringing together two tetravalent cations, which at the low doping levels considered above only exist in small concentration.

#### V. SUMMARY

We have derived a series of temperature-independent relations for the Seebeck coefficient appropriate to transition-metal-oxide perovskites with highest electronic occupation lying in the transition metal  $t_{2g}$  states. Derivation of these relations is obtained using an approach that explicitly treats the spin and orbital degeneracies associated with electronic occupation of these states. Separate relations apply depending upon whether the Coulomb repulsion energy  $U$  between aligned electrons in different  $t_{2g}$  orbitals at the same site is



large or small compared to typical thermal energies. These forms are not applicable to the extreme high-temperature limit in which the average thermal energies have values comparable to the true Hubbard energies, i.e., the energies between electrons of opposite spin in the same orbital. They are valid, however, for the range of temperatures encountered in many reported experimental Seebeck coefficient measurements. In each of the limiting cases considered we have derived separate expressions that apply in the limits of strong and weak magnetic coupling between spins in adjacent sites. Our expressions, evaluated with no adjustable parameters, are in very good agreement with reported Seebeck coefficient measurements for the  $\text{La}_{1-x}\text{Sr}_x\text{CrO}_3$  series and suggest that at all temperatures reported the magnetic coupling is sufficiently weak to allow considerable spin degeneracy in these systems. It should be possible to extend the approach pre-

sented in this paper to allow analysis of transition-metal oxides having their highest occupied electronic states lying in the doubly degenerate higher-energy  $e_g$  manifold. Complicating this extension is the fact that with electronic occupation of the  $e_g$  levels there is still a spin degeneracy associated with filled  $t_{2g}$  levels.

#### ACKNOWLEDGMENTS

This work was supported in part by the Basic Energy Sciences Division of the Department of Energy through Grant No. DE-FG0285ER45219 and through a grant from the University of Missouri Research Board. One of the authors (P.E.P.) thanks Professor D. Emin for extended discussions on subjects related to those discussed in this paper and in particular for bringing to his attention the work in Ref. 15.

- <sup>1</sup>R. Raffaele, H.U. Anderson, D.M. Sparlin, and P.E. Parris, *Phys. Rev. B* **43**, 7991 (1990).
- <sup>2</sup>R. Raffaele, H.U. Anderson, D.M. Sparlin, and P.E. Parris, *Phys. Rev. Lett.* **65**, 1383 (1990).
- <sup>3</sup>R. Raffaele, J.S. Shapiro, H.U. Anderson, P.E. Parris, and D.M. Sparlin, *Ceram. Trans.* **24**, 239 (1991).
- <sup>4</sup>M.J. DeBarr, H.U. Anderson, M.M. Nasrallah, D.M. Sparlin, P.E. Parris, and R. Raffaele, *Ceram. Trans.* **24**, 229 (1991).
- <sup>5</sup>J.H. Kuo, H.U. Anderson, and D.M. Sparlin, *J. Solid State Chem.* **83**, 52 (1989); **87**, 55 (1990).
- <sup>6</sup>J.H. Kuo, Ph.D. thesis, The University of Missouri–Rolla, 1987 (unpublished).
- <sup>7</sup>C.J. Yu, H.U. Anderson, and D.M. Sparlin, *J. Solid State Chem.* **78**, 242 (1989).
- <sup>8</sup>D.P. Karim and A.T. Aldred, *Phys. Rev. B* **20**, 2255 (1979).
- <sup>9</sup>J.B. Webb, M. Sayer, and A. Mansingh, *Can. J. Phys.* **55**, 1725 (1977).
- <sup>10</sup>W.J. Weber, C.W. Griffin, and J.L. Bates, *J. Am. Ceram. Soc.* **70**, 2656 (1987); *J. Mater. Res.* **1**, 2656 (1986).
- <sup>11</sup>G.F. Carini, H.U. Anderson, M.M. Nasrallah, and D.M. Sparlin, *J. Solid State Chem.* **94**, 329 (1991); *Solid State Ionics Diffusion Reactions* **49**, 233 (1991).
- <sup>12</sup>J.W. Stevenson, M.M. Nasrallah, H.U. Anderson, and D.M. Sparlin, *J. Solid State Chem.* **102**, 175 (1993).
- <sup>13</sup>S.R. Sehlin, H.U. Anderson, and D.M. Sparlin, *Solid State Ionics Diffusion Reactions* **78**, 235 (1995); *Phys. Rev. B* **52**, 11 681 (1995).
- <sup>14</sup>J.B. Goodenough, *Prog. Solid State Chem.* **5**, 145 (1971); J.B. Goodenough, *Phys. Rev.* **164**, 785 (1967); J.B. Goodenough, *Magnetism and The Chemical Bond* (Wiley, New York, 1963).
- <sup>15</sup>R.R. Heikes, in *Transition Metal Compounds*, edited by E.R. Schatz (Gordon and Breach, New York, 1963), p. 1.
- <sup>16</sup>R.R. Heikes, A.A. Maradudin, and R.C. Miller, *Ann. Phys. (Paris)* **8**, 783 (1963); R.R. Heikes, in *Thermoelectricity*, edited by R. Heikes and R. Ure (Interscience, New York, 1961), Chap. 4.
- <sup>17</sup>P.M. Chaikin and G. Beni, *Phys. Rev. B* **13**, 647 (1976).
- <sup>18</sup>D. Emin, *Phys. Rev. Lett.* **35**, 882 (1975).
- <sup>19</sup>It is worth pointing out, in this context, that many subsequent extensions of what is generally referred to in the literature as “Heikes’s formula,” involve contributions to the transport entropy that were identified by Heikes. See, e.g., Ref. 15.
- <sup>20</sup>J.P. Doumerc, *J. Solid State Chem.* **110**, 419 (1994).
- <sup>21</sup>N. Tsuda, K. Nasu, A. Yanase, and K. Siratori, *Electronic Conduction in Oxides* (Springer-Verlag, Berlin, 1991), Chap. 2.
- <sup>22</sup>D.J. Lam and B.W. Veal, *Phys. Rev. B* **22**, 5730 (1980).
- <sup>23</sup>C.A. Domenicali, *Rev. Mod. Phys.* **26**, 237 (1954).
- <sup>24</sup>L. Onsager, *Phys. Rev.* **37**, 405 (1931); **38**, 2265 (1931).
- <sup>25</sup>H.B.G. Casimir, *Rev. Mod. Phys.* **1** **7**, 343.
- <sup>26</sup>S.R. DeGroot, *Thermodynamics of Irreversible Processes* (Interscience, New York, 1951), Chap. 2.
- <sup>27</sup>R. Kubo, *J. Phys. Soc. Jpn.* **12**, 570 (1957); *Rep. Prog. Phys.* **29**, 255 (1966); in *Lectures in Theoretical Physics*, edited by W. Brittin (Interscience, New York, 1959), Vol. 1, p. 120.
- <sup>28</sup>J.M. Luttinger, *Phys. Rev.* **135**, A1505 (1964).
- <sup>29</sup>D.B. Marsh, Ph.D. thesis, The University of Missouri–Rolla, 1995 (unpublished).
- <sup>30</sup>N.L. Liu and D. Emin, *Phys. Rev. B* **30**, 3250 (1984); **32**, 2285 (1985).
- <sup>31</sup>T. Holstein, *Ann. Phys. (N.Y.)* **8**, 325 (1959); **8**, 343 (1959).
- <sup>32</sup>D. Emin and T. Holstein, *Ann. Phys. (N.Y.)* **53**, 439 (1969).
- <sup>33</sup>D. Emin, *Adv. Phys.* **24**, 305 (1975); *Phys. Rev. Lett.* **32**, 303 (1974).
- <sup>34</sup>E.J.W. Verwey, P.W. Haaijman, F.C. Romeijn, and G.W. van Oosterhout, *Philips Res. Rep.* **5**, 173 (1950).
- <sup>35</sup>K.P. Bansal, S. Kumari, B.K. Das, and G.C. Jain, *J. Mater. Sci.* **18**, 2095 (1983).
- <sup>36</sup>S.T. Song, H.Y. Pan, Z. Wang, and B. Yang, *Ceram. Int.* **10**, 143 (1984).